Experimental investigation of Brillouin and Raman scattering in a 2SG sulfide glass microstructured chalcogenide fiber

C. Fortier[1], J. Fatome[1], S. Pitois[1], F. Smektala[1], G. Millot[1], J. Troles[2], F. Desevedavy[2], P. Houizot[2] L. Brilland[3] and N. Traynor[3]

[1]*Institut Carnot de Bourgogne (ICB), UMR-CNRS 5209, Université de Bourgogne, 9 av. Alain Savary, 21078 Dijon, France*
[2]*Laboratoire Verres et Céramiques (LVC), UMR-CNRS 6226, Université de Rennes I, Campus de Beaulieu, 35042 Rennes, France*
[3]*PERFOS, 11 rue de Broglie, 22300 Lannion, France*
Corresponding author: jfatome@u-bourgogne.fr

Abstract: In this work, we investigate the Brillouin and Raman scattering properties of a $Ge_{15}Sb_{20}S_{65}$ chalcogenide glass microstructured single mode fiber around 1.55 µm. Through a fair comparison between a 2-m long chalcogenide fiber and a 7.9-km long classical single mode silica fiber, we have found a Brillouin and Raman gain coefficients 100 and 180 larger than fused silica, respectively.

©2008 Optical Society of America

OCIS codes: (060.4370) Nonlinear optics, fibers; (290.5900) Scattering, stimulated Brillouin; (060.2270) Fiber characterization; (190.5650) Raman effect.

References and links

1. G. P. Agrawal, *Nonlinear Fiber Optics*, 3th Ed (Academic Press, Boston, 2001).
2. M. O. Deventer and A. J. Boot, "Polarization Properties of Stimulated Brillouin Scattering in Single-Mode Fibers," J. Lightwave Technol. **12**, 585-590 (1994).
3. K. S. Abedin, "Brillouin amplification and lasing in a single-mode As_2Se_3 chalcogenide fiber," Opt. Lett. **31**, 1615-1617 (2006).
4. K. Y. Song, K. S. Abedin, K. Hotate, M. González Herráez, and L. Thévenaz, "Highly efficient Brillouin slow and fast light using As_2Se_3 chalcogenide fiber," Opt. Express **14**, 5860-5865 (2006).
5. C. Jáuregui, H. Ono, P. Petropoulos, and D. J. Richardson, "Four-fold reduction in the speed of light at practical power levels using Brillouin scattering in a 2-m Bismuth-oxide fiber," in Proc. Optical Fiber Communications Conference (OFC2006), Piscataway USA, March 2006, PDP2 (Postdeadline paper).
6. N. Sugimoto, T. Nagashima, T. Hasegawa, S. Ohara, K. Taira, and K. Kikuchi, "Bismuth-based optical fiber with nonlinear coefficient of $1360W^{-1}km^{-1}$," in Proc. Optical Fiber Communications Conference (OFC2004), Anaheim USA, March 2004, PDP26 (Postdeadline paper).
7. F. Smektala, C. Quemard, L. Leneindre, J. Lucas, A. Barthélémy, and C. De Angelis, "Chalcogenide glasses with large non-linear refractive indices," J. Non-Cryst. Solids **239**, 139-142 (1998).
8. L. fu, V. G. Ta'eed, E. C. Mägi, I. C. M. Littler, M. D. Pelusi, M. R. E. Lamont, A. Fuerbach, H. C. Nguyen, D. Y. Yeom, and B. Eggleton, "Highly nonlinear chalcogenide fibres for all-optical signal processing," Opt. Quantum Electron. 10.1007/s11082-007-9180-7 (2008).
9. K. S. Abedin, "Observation of strong stimulated Brillouin scattering in single-mode As2Se3 chalcogenide fiber," Opt. Express **13**, 10266-10271 (2005).
10. C. Florea, M. Bashkansky, Z. Dutton, J. Sanghera, P. Pureza, and I. Aggarwal, "Stimulated Brillouin scattering in single-mode As_2S_3 and As_2Se_3 chalcogenide fibers," Opt. Express **14**, 12063-12070 (2006).
11. O. P. Kulkarni, C. Xia, D. J. Lee, M. Kumar, A. Kuditcher, M. N. Islam, F. L. Terry, M. J. Freeman, B. G. Aitken, S. C. Currie, J. E. McCarthy, M. L. Powley, and D. A. Nolan, "Third order cascaded Raman wavelength shifting in chalcogenide fibers and determination of Raman gain coefficient," Opt. Express **14**, 7924-7930 (2006).
12. F. Smektala, F. Desevedavy, L. Brilland, P. Houizot, J. Troles, **and** N. Traynor, "Advances in the elaboration of chalcogenide photonic crystal fibers for the mid infrared," SPIE **6588,** (2007).
13. L. Brilland, F. Smektala, G. Renversez, T. Chartier, J. Troles, T. N. Nguyen, N. Traynor, and A. Monteville "Fabrication of complex structures of Holey Fibers in chalcogenide glasses," Opt. Express **14** (3) 1280-5 (2006).

14. J. Fatome, S. Pitois, and G. Millot, "20-GHz-to-1-THz repetition rate pulse sources based on multiple four-wave mixing in optical fibers," IEEE J. Quantum Electron. **42**, 1038-1046 (2006).
15. S. Pitois, C. Finot, J. Fatome, B. Sinardet, and G. Millot, "Generation of 20-GHz picosecond pulse trains in the normal and anomalous dispersion regimes of optical fibers," Opt. Commun. **260**, 301-306 (2006).

1. Introduction

Brillouin and Raman scattering effects are famous phenomena of both fundamental and applicative interests. For almost a century, they have been studied in a large number of media, leading to numerous applications in the field of optical physics [1-11]. For example, these effects were found to be very useful to amplify with very low noise a small optical signal [1, 3], to design fiber-based lasing systems [1, 3] as well as to generate tunable delay lines via slow and fast light processes [4-5]. For most of these applications, it may be desirable to found a medium with a large nonlinear efficiency in order to decrease the required input power as well as to compact the set-up, thus improving the stability of the system with respect to undesirable effects such as chromatic dispersion, polarization sensitivity or parameter fluctuations along the fiber length. To this aim, several fibered media, such as Bismuth oxide fibers [5-6] or Chalcogenide fibers [7-8], exhibiting very large nonlinearities have been studied in recent works. Chalcogenide glass fiber was found to be an excellent candidate for nonlinear applications [8] thanks to a nonlinear index over two to three orders of magnitude stronger than in standard fused silica fiber [7-8]. In other previous studies, the strong nonlinear interest of chalcogenide fibers was also underlined through the characterization of Brillouin and Raman gains which were measured to be ~150 and ~89 times larger than that of fused silica, respectively [9-11]. In this work, we investigate for the first time to our knowledge the Brillouin and Raman scattering properties of a strong nonlinear microstructured chalcogenide fiber based on a $Ge_{15}Sb_{20}S_{65}$ germanium sulfide glass. By means of a comparative experimental study with a standard fused silica fiber, we have found that the Brillouin and Raman gain coefficients in the microstructured chalcogenide fiber are about ~100 and ~180 times larger than fused silica, with frequency shifts equal to 8.5 GHz and 9.7 THz, respectively. Finally, thanks to an auto-heterodyne detection set-up, we have measured a Brillouin gain linewidth of 10 MHz, in good agreement with previous estimations.

2. Microstructured Chalcogenide Fiber

The microstructured chalcogenide fiber was designed and drawn at the University of Rennes 1 following the technique of stack and draw. The chalcogenide base glass chosen for the fiber elaboration is a germanium sulfide glass modified by antimony. Its nominal composition is $Ge_{15}Sb_{20}S_{65}$ and is transparent from around 600 nm to 11 μm. This type of glasses has been demonstrated to be suitable for the elaboration of microstructured fibers by the stack and draw process [12]. After synthesis of the nominal glass in silica ampoules sealed under vacuum, tubes of 12 mm outer diameter are obtained by centrifugation of the ampoule. One of them is then stretched on a drawing tower in order to reduce its diameter to around 600 nm. Capillaries are cut from this stretched tube and are stacked in a hexagonal configuration exhibiting three rounds of holes around a central glass rod of the same glass composition. The stack is jacketed by another external glass tube. This preform is finally drawn on a drawing tower through a careful control of the gas pressure inside it. A pretty and regular microstructure is obtained by this way (Fig. 1).
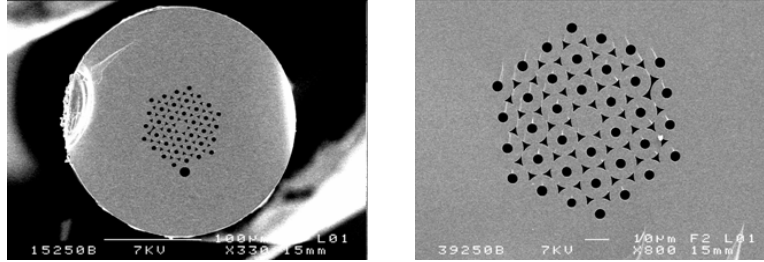
Fig. 1. Pictures of the section of the $Ge_{15}Sb_{20}S_{65}$ chalcogenide glass microstructured optical fiber elaborated by the stack and draw process.

The fiber has been firstly characterized from the point of view of its linear optical characteristics. The losses, measured by the cut back technique, are found to 5.5 dB/m at 1.55 µm. The pitch Λ is 13.3 µm and the d/Λ ratio is 0.3 at 1.55 µm corresponding to a single mode behaviour which has been experimentally verified despite the presence of interstitial holes between the stacked capillaries. The mode field diameter is around 8 µm at 1.55 µm and the effective area of the waveguide is 50 µm².

3. Brillouin characterization

Figure 2 illustrates the experimental set-up used to characterize the Brillouin properties of the $Ge_{15}Sb_{20}S_{65}$ microstructured chalcogenide fiber. A continuous wave (cw) is first generated around 1552 nm by means of a distributed feedback (DFB) laser diode having a spectral linewidth given by the manufacturer of 150 kHz. Thanks to an acousto-optical switch (AO), we then convert this cw into a 140-ns quasi Gaussian pulse train at a repetition rate of 500 kHz. The pulse train is then amplified by means of an erbium doped fiber amplifier (EDFA) at an average power of 30 dBm. A variable attenuator, associated with a 90:10 coupler and a Power Meter (PwM) are then used to adjust the injected average power into the fiber. Finally, the resulting signal is launched into a circulator whose port #2 is used to inject the incident light into the fiber under-test and port #3 to collect the backscattered light. The intensity of the Brillouin Stokes component is then measured at port #3 thanks to an optical spectrum analyzer (OSA) having a spectral resolution of 0.02 nm (2.5 GHz). In order to complete a comparative study, the same experimental protocol was performed successively in a reference fiber and in our chalcogenide fiber. The reference fiber was a L=7.9-km long classical fused silica single mode fiber (SMF28) with losses of α_{dB}=0.25dB/km=4.343α leading to an effective length L_{eff}=$[1-exp(-\alpha L)]/\alpha$ of 6.35 km whereas the chalcogenide fiber was a 2-m long microstructured $Ge_{15}Sb_{20}S_{65}$ fiber having an effective length of 0.7 m (5.5 dB/m). Note that the input signal was coupled into the chalcogenide fiber by means of an optical fiber splicer which permits an efficient fiber coupling with losses around 2.5 dB.
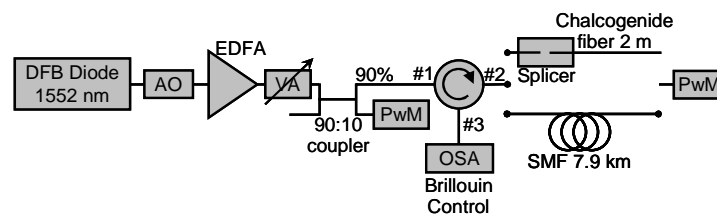

Fig. 2. Experimental set-up for Brillouin characterization.

Figure 3 shows a typical backscattered optical spectrum obtained for the two types of fibers. In dashed line, we can observe the classical Brillouin spectrum obtained in the 7.9-km long SMF fiber. A high power backscattered Stokes Brillouin component localized around -11 GHz is clearly visible, in good agreement with values reported in the literature [1]. In solid line, we can see the Brillouin spectrum obtained with the 2-m long microstructured

chalcogenide fiber. The Brillouin component is now generated with a smaller shift of -8.2 GHz which is close to the -7.95 GHz value obtained by Abedin in a single mode As_2Se_3 fiber [9].
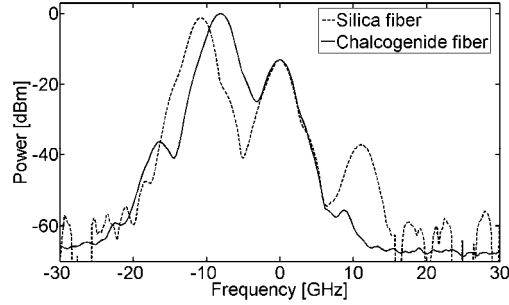

Fig. 3. Experimental Brillouin spectrum recorded at port #3 of the circulator for the 7.9-km long SMF (dashed line) and 2-m long chalcogenide fiber.

In order to determine the threshold and gain of the Brillouin scattering, we have recorded the transmitted and backscattered Brillouin component powers as a function of the injected power. Figure 4(a) sums up the results obtained in the 7.9-km long SMF fiber. We can clearly observe a typical Brillouin behaviour with an exponential growth of the amount of energy backscattered into the fiber as well as a quasi saturation of the transmitted power. The Brillouin threshold P_{th}, usually defined as the power leading to an amount of backscattered energy equal to the transmitted one [1], corresponds here to a threshold value of 50 mW. The Brillouin gain g_B was then calculated by means of the following relation [1]:

$$g_B K P_{th} L_{eff} / A_{eff} \approx 21 \tag{1}$$

where A_{eff} is the effective area and K a constant that depends on the polarization properties of the fiber under-test, $K=2/3$ for a standard single mode fiber and $K=1$ for polarization maintaining fiber [2]. By taking $P_{th}= 50$ mW, $A_{eff} = 80$ µm² and $K=2/3$, we have calculated a Brillouin gain of $g_B=8.10^{-12}$ m/W for the SMF fiber which is in the order of magnitude of the values usually reported in the literature [1]. The Brillouin figure of merit defined by Song *et al.* in ref. [4] *FOM=G/[P_{pump}.L_{eff}.n]* where *G, P_{pump}* and *n* are the Brillouin gain in dB, the corresponding pump power and the refractive index, was found to be 6.10^{-5} dB/mW/m for the SMF (*G*=70 dB, P_{pump}=130 mW. and *n*=1.45).

   Figure 4(b) shows the results obtained with the chalcogenide fiber. The behaviour is similar to the one observed in the SMF fiber, with much higher powers. The birefringence of the chalcogenide fiber was measured to 1 ps/m and special care was taken to inject the initial signal along one of the axis of the fiber. By taking $K=1$ in expression (1), the Brillouin threshold was measured to be $P_{th} = 1.95$ W, corresponding to a Brillouin gain of $g_B=8.10^{-10}$ m/W that is to say 100 more than in the previous silica fiber. This value is smaller than in refs. [9-10] but could be explained by the definition of the Brillouin threshold used in this reference. The corresponding FOM was found to be 5.10^{-3} dB/mW/m (*G*=55 dB, P_{pump}=6.5 W. and *n*=2.25) which is 80 times larger than the SMF fiber in concordance with results obtained in ref. [4] (x 110).
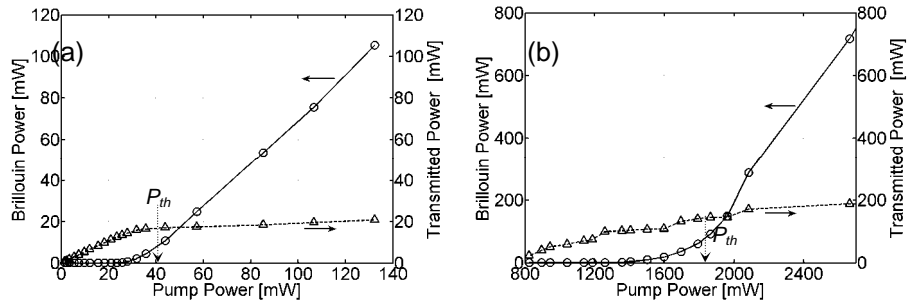
Fig. 4. Backscattered and transmitted powers as a function of the input power (a) SMF (b) Chalcogenide fiber.

Finally, we have measured the linewidth of the Brillouin-gain thanks to the auto-heterodyne set-up schematized in Fig. 5(a). The backscattered signal with a Brillouin/residual-pump intensity ratio larger than 15 dB is injected into an interferometer whose arms are decorelated thanks to 4.5 km of SMF fiber and frequency-shifted by 80 MHz by means of two 40-MHz-shift acousto-optics with opposite sign shift (AO+ and AO-). The resulting beat-signal is finally detected by a photodetector and analyzed in frequency owing to a RF analyzer having a spectral resolution of 100 kHz. Figure 5(b) shows the experimental results. The dotted line represents the initial DFB diode spectrum, with a measured 3dB linewidth of 1.6 MHz. This value is much larger than those given by the manufacturer (150 kHz) and is attributed to the rapid wavelength fluctuations due to the absence of thermal regulation. Meanwhile, the diode linewidth remains one order of magnitude smaller than the Brillouin-gain linewidth. The dashed line corresponds to the 7.9-km SMF Brillouin signal which linewidth was found to be 12.6 MHz in good agreement with the literature [1]. More surprisingly, the shape is closer to a Gaussian than a Lorentzian. This phenomenon could be explained by the mechanical winding and the long length of the fiber which inhomogeneities could distort and broaden slightly the Brillouin gain curve. Finally, the solid line shows the Brillouin-gain obtained with the chalcogenide fiber. We observed a Brillouin gain spectrum with a Lorentzian-look shape and a bandwidth of 9.5 MHz which is slightly smaller than in ref. [9], presumably due to the different glass composition and the presence of the microstructure.
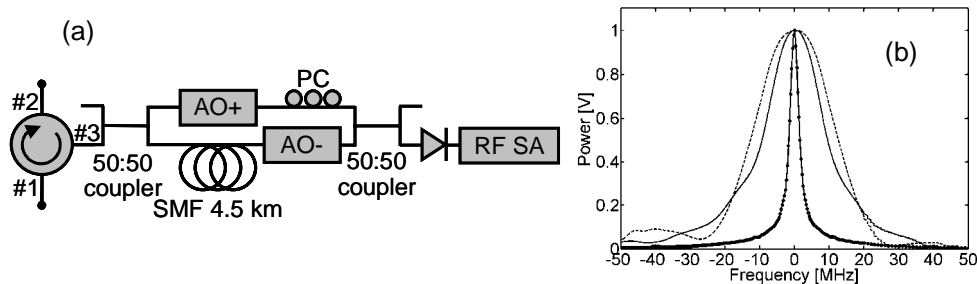

Fig. 5. Experimental set-up of the Brillouin auto-heterodyne detection. RF spectrum of the input DFB Diode (dotted line), SMF (dashed line) and chalcogenide Brillouin backscattered signal (solid line).

4. Raman characterization

Next, we have focused our attention on the Raman scattering effect occurring in the same $Ge_{15}Sb_{20}S_{65}$ microstructured chalcogenide and SMF fibers. Figure 6 shows the experimental set-up. A 1-kHz 10-ns square pulse laser emitting around 1553 nm is used as Raman pump. In order to determine the Raman gain, we have measured the amplification undergone by a seed-signal injected in a co-propagation configuration and shifted from the Raman pump by 100 nm for the SMF and by 83 nm for the chalcogenide fiber (see below). The seed components

were obtained through a multiple four-wave mixing process taking place into a highly non-linear fiber (HNLF) [13-14]. To this end, an initial beat signal was first generated from the superposition of two cws emitted by two external cavity lasers (ECL) separated from 1 THz and centred around 1560 nm. This beat signal, amplified at an average power of 30 dBm thanks to an EDFA, was then injected into a 500-m long HNLF fiber from *OFS* with an anomalous dispersion of 0.5 ps/km.nm. Thanks to the combined effects of Kerr nonlinearity and anomalous dispersion, a broad frequency-comb is finally generated at the fiber output [13-14]. Figure 7(a) shows the output HNLF spectrum with the two sidebands localized around 1636 nm and 1653 nm which were used as Raman seeds. At the output of the fiber under-test, only the part of the signal wave which has been amplified was injected into the optical spectrum analyzer (OSA) thanks to an acousto-optic (AO) synchronised on the Raman pump. In the case of the 1.5-m long microstructured chalcogenide fiber, signals were coupled at the input and output of the fiber by means of two optical fiber splicers with coupling losses of 2.5 dB.
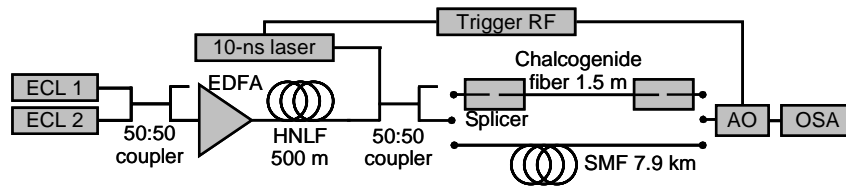

Fig. 6. Experimental set-up for Raman characterization.

The Raman properties of the chalcogenide fiber were first characterized in spontaneous regime without the 1636-nm seeding. Figure 7(b) illustrates the spontaneous Raman response occurring into the chalcogenide fiber for an input pump power of 80 W. The Raman detuning was measured at 83 nm (9.7 THz) with a FWHM of 5.5 nm. Note that any spontaneous Raman emission was detected at the output of the 7.9-km long SMF fiber (dashed-line). In stimulated regime, we have first measured the power of the output 1653-nm amplified signal as a function of the input Raman pump power P_{pump} for the 7.9-km long SMF fiber. As can be seen in Fig. 7(c), a strong amplification of the input signal was observed with a maximum gain close to $G = 49$ dB. This value corresponds to a gain per unit length of 6.10^{-3} dB/m and a Raman gain of $g_R=ln(G).A_{eff}/P_{pump}.L_{eff}=1.10^{-13}$ m/W, in good agreement with usual values of literature [1]. The inset of Fig. 7(c) shows a typical spectrum of the 1653-nm amplified signal recorded for a pump power of 900 mW. The same experiment was then completed with the 1.5-m microstructured chalcogenide fiber by means of the 1636-nm seed component. The amplification of the 1636-nm input signal is shown in Fig. 7(d). The maximum gain of 37 dB corresponds to a gain per unit length of 24.7 dB/m and a Raman gain of $g_R=1.8.10^{-11}$ m/W, that is to say 180 times larger than the above value of the fused silica fiber and three-fold higher than the previous result of ref. [10]. Finally, the inset in Fig. 7(d) illustrates a typical amplified signal spectrum recorded for a pump power of $P_{pump} = 24.5$ W.
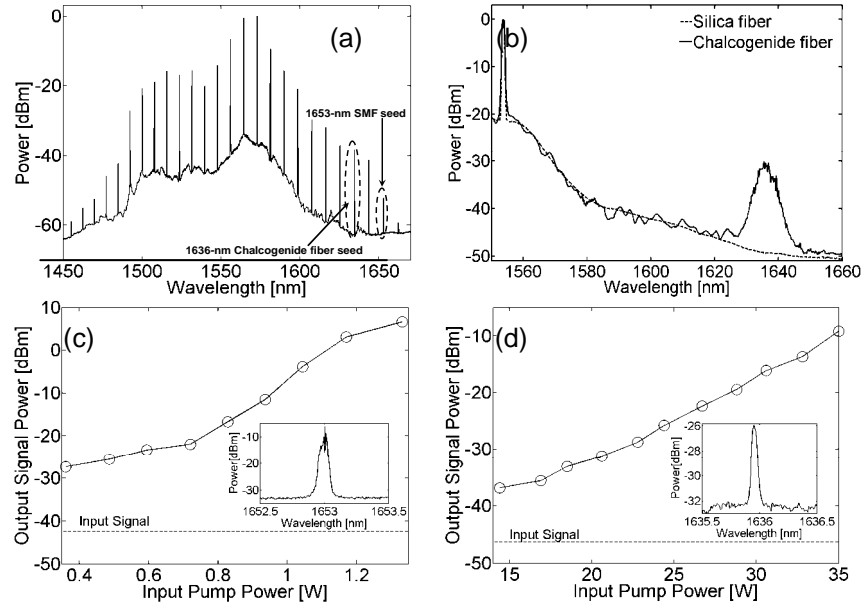
Fig. 7. (a) Optical spectrum of the frequency comb generated by multiple four wave mixing in the HNLF. (b) Spontaneous Raman scattering at the output of the 7.9-km long SMF (dashed line) and chalcogenide fiber (solid-line) for an input pump power of 80 W. (c) Output signal power as a function of input pump power for the 7.9-km long SMF fiber. Inset: Output amplified signal spectrum for a pump power of 0.9 W (d) Output signal power as a function of input pump power for the chalcogenide fiber. Inset: Output amplified signal spectrum for a pump power of 24.5 W.

5. Conclusion

In this work, we have investigated for the first time of our knowledge the Brillouin and Raman properties of a microstructured $Ge_{15}Sb_{20}S_{65}$ chalcogenide glass single mode fiber around 1.55 µm. By means of a fair experimental comparison between a 7.9-km long standard silica single mode fiber and the 2-m long microstructured chalcogenide fiber, we have found a Brillouin and Raman gain coefficient of $g_B=8.10^{-10}$ m/W and $g_R=1.8.10^{-11}$ m/W corresponding to 100 and 180 times larger than those of fused silica for a frequency shift of 8.2 GHz and 9.7 THz, respectively. Moreover, thanks to an auto-heterodyne detection set-up, we have measured a Brillouin gain bandwidth of 9.5 MHz. Finally, we believe that this kind of fiber which already presents nonlinearity properties two orders of magnitude larger than fused silica and which could be over enhanced by increasing the field confinement by means of a microstructure reduction could find many applications in the field of nonlinear optical physics and in particular for the implementation of optical processing functions into a compact form.

Acknowledgments